Biomaterials Science

PAPER

View Article Online
View Journal | View Issue

Cite this: *Biomater. Sci.*, 2018, **6**, 2487

Injectable dynamic covalent hydrogels of boronic acid polymers cross-linked by bioactive plant-derived polyphenols†

Zhuojun Huang, ‡[a] Peyman Delparastan, ‡[a] Patrick Burch, [b] Jing Cheng, [b] Yi Cao [c] and Phillip B. Messersmith *[a,b,d]

Received 25th April 2018,
Accepted 9th May 2018

DOI: 10.1039/c8bm00453f

rsc.li/biomaterials-science

We report here the development of hydrogels formed at physiological conditions using PEG (polyethylene glycol) based polymers modified with boronic acids (BAs) as backbones and the plant derived polyphenols ellagic acid (EA), epigallocatechin gallate (EGCG), tannic acid (TA), nordihydroguaiaretic acid (NDGA), rutin trihydrate (RT), rosmarinic acid (RA) and carminic acid (CA) as linkers. Rheological frequency sweep and single molecule force spectroscopy (SMFS) experiments show that hydrogels linked with EGCG and TA are mechanically stiff, arising from the dynamic covalent bond formed by the polyphenol linker and boronic acid functionalized polymer. Stability tests of the hydrogels in physiological conditions revealed that gels linked with EA, EGCG, and TA are stable. We furthermore showed that EA- and EGCG-linked hydrogels can be formed *via in situ* gelation in pH 7.4 buffer, and provide long-term steady state release of bioactive EA. *In vitro* experiments showed that EA-linked hydrogel significantly reduced the viability of CAL-27 human oral cancer cells *via* gradual release of EA.

Introduction

Plant polyphenols are a family of naturally derived compounds that contain a high concentration of phenolic hydroxyl groups and are linked to diverse biological functions such as chemical defense, pigmentation, structural support, and prevention of radiation damage.[1,2] In addition to their recent emergence as building blocks for functional materials,[3–6] plant polyphenols are highly celebrated for their complex bioactivities and antioxidant behavior. A high dietary intake of polyphenols has been linked to a reduced incidence of a number of diseases, including cancer, diabetes, osteoporosis as well as cardiovascular and neurodegenerative diseases, and several polyphenols have been investigated as therapeutics.[7–10] For instance, ellagic acid (EA) has anti-proliferative properties and has been shown effective against prostatic, breast, brain, and oral cancers in a number of *in vitro* and small-animal models.[11–16] In addition to antiproliferative effects, many polyphenols like epigallocatechin gallate (EGCG) and tannic acid (TA) have been found to have antioxidant, antibacterial, and anti-inflammatory effects.[7] However, despite their impressive therapeutic effects, polyphenols suffer from a number of drawbacks which limit their clinical translation, including poor bioavailability, rapid metabolism, and poor membrane permeability. Therefore, development of an efficient delivery method for these beneficial therapeutic molecules would be a milestone in translation into the clinic.

Recently, dynamic covalent chemistry has been explored to develop hydrogels with predictable degradation and drug release kinetics that exploit the stimuli-responsive nature of the complexes formed *via* dynamic covalent chemistry.[17–19] One example is given by boronic esters formed between boronic acids and *cis*-1,2 or *cis*-1,3 diol containing molecules.[20–24] Boronic acids have been proved to be stable in biological conditions and have no or extremely little toxicity on the human body.[25–27] Moreover, the equilibrium between boronic acid and boronic ester is sensitive towards pH, temperature, and competing hydroxylated compounds present in the media,[20,21,28,29] enabling the formation of novel local drug delivery systems and hydrogels with mechanical properties that are responsive to changes in pH.[18,22,25,30–35] Although boronate ester complexes are generally favored at alkaline pH, the equilibrium can be tuned by modification of the chemical structure of the boronic acid group.[36–39] Using this approach it

[a]*Department of Materials Science and Engineering, University of California, Berkeley, Berkeley, CA, 94720-1760, USA. E-mail: philm@berkeley.edu*
[b]*Department of Bioengineering, University of California, Berkeley, Berkeley, CA, 94720-1760, USA*
[c]*Department of Physics, Nanjing University, Nanjing, 210093, China PR*
[d]*Materials Science Division, Lawrence Berkeley National Laboratory, Berkeley, CA, USA*

†Electronic supplementary information (ESI) available. See DOI: 10.1039/c8bm00453f

‡These authors contributed equally.

is possible in principle to shift the equilibrium in favor of the boronate ester to neutral pH, affording the ability to form hydrogels from boronic acid derivatized polymers under physiological conditions.[36] Since the polyphenols are susceptible to oxidation and oligomerization at highly alkaline pH,[3] lowering the complexation pH can further result in sustained bioactivity of these molecules due to limited oxidation.

Although the high hydroxyl content and rich bioactivity spectrum of polyphenols presents a unique opportunity to form therapeutically active dynamic covalent hydrogels with boronic acid polymers, these molecules have not been widely investigated in this context. Herein we exploit the pH dependence and dynamic nature of complexes between boronic acid functionalized PEG and polyphenols as bioactive injectable hydrogels (Fig. 1). In this concept, the polyphenol functions both as cross-linker and therapeutic, forming a hydrogel by injection of a precursor solution of polymer and polyphenol that solidifies through formation of boronate ester cross-links upon neutralization to physiologic pH. The dynamic nature of the boronate ester bond provides a mechanism for latent hydrogel disassembly and release of therapeutic polyphenols into the surrounding environment.[37,38,40] Numerous combinations of natural polyphenols, substituted boronic acids and PEG polymers of different architecture were screened by rheological analysis, revealing several formulations that gave rise to rapid gelation at physiologic pH. Insight into the molecular mechanics of boronic acid–polyphenol interactions was provided by measuring bond rupture forces in a pH dependent manner using single molecule force spectroscopy (SMFS). Finally, we studied the kinetics of EA release from a PEG–boronic acid hydrogel and demonstrated the *in vitro* cytotoxic effects of released EA on cancer cells.

Experimental

Materials

4-Arm PEG (pentaerythritol core, M.W. 10 kDa) (PEG4P) and 8-arm PEG (tripentaerythritol core, M.W. 20 kDa) (PEG8T) with hydroxyl endgroups were purchased from Creative PEGWorks. PEG8T and 8-arm PEG-NH_2 (hexaglycerol core, M.W. 20 kDa) (PEG8H) with amine endgroups were obtained from JenKem Technology. (4-(2-Aminoethyl) phenyl) boronic acid (BA1) and 3-carboxy-5-nitrophenylboronic acid (BA4) were obtained from Sigma-Aldrich. 3-Amino-5-nitrophenylboronic acid (BA2) was purchased from Alfa Aesar and 6-nitrobenzo [*c*][1,2] oxaborol-1(3*H*)-ol was from Ark Pharm. 2,2,6,6-Tetramethyl-1-piperidinyloxy, free radical, 2,2,6,6-tetramethylpiperidine 1-oxyl (TEMPO), NaClO, 2-(1*H*-benzotriazol-1-yl)-1,1,3,3-tetramethyluronium hexafluorophosphate (HBTU), triethylamine (TEA), Pd on charcoal, *N*,*N*-diisopropylethylamine (DIPEA), *N*,*N*-diisopropylcarbodiimide (DIC), hydroxybenzotriazole (HOBt), EA, EGCG, TA, NDGA, rutin trihydrate and other polyphenols and chemicals used for PEG modification were acquired from Sigma-Aldrich. Fetal bovine serum (FBS), phosphate buffered saline (PBS) buffer, Dulbecco's Modified Eagle Medium (DMEM) with glutamine and pyruvate were purchased from Invitrogen. CAL-27 human squamous cell carcinoma cells were purchased from American Type Culture Collection (ATCC).

Polymer synthesis

A modular approach was adopted whereby PEGs of different molecular weights and architectures were functionalized with four different phenylboronic acids (Fig. 1c). The pK_a values of the BAs used range from 6.9 to 9.0 based on previous

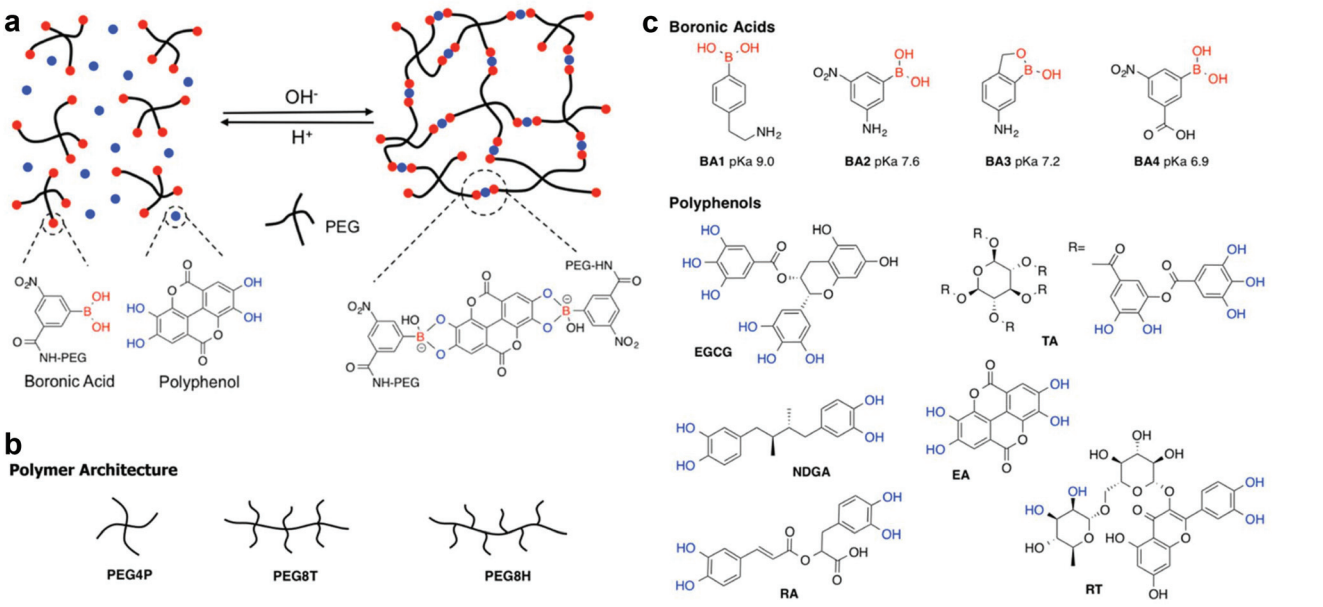

Fig. 1 (a) Schematic illustration of pH responsive complexation between boronic acid functionalized PEG and polyphenols resulting in formation of a hydrogel network. The specific boronate ester formed between BA4 and EA is shown as an example only. Architectures of PEG polymers (b), and chemical structures of boronic acids and polyphenols (c) used in the experiments. Vicinal diols capable of boronate ester formation are shown in blue.

studies.[39,41–45] Detailed synthesis methods and NMR spectra of all PEG products can be found in ESI (Fig. S1–S10†). PEG-OH was converted to PEG-COOH by TEMPO and NaClO and then reacted with the primary amine on BA1, BA2 and BA3 using HBTU and TEA. BA4 was linked to PEG-NH_2 using DIPEA, DIC and HOBt.

Hydrogel formation

A typical procedure used to form hydrogels was as follows: 50 mg of polymer was dissolved in pH 7.4 PBS buffer (10 mM PO_4^{3-}, 137 mM NaCl, and 2.7 mM KCl) and mixed with solutions of polyphenol in the PBS buffer. In a few cases for polyphenols with limited solubility in water, DMSO was used to dissolve the polyphenol (Table 2). The molecular ratio between boronic acid groups on the polymer chain and active diol moiety on polyphenol linker was kept constant at 1 to 1 ratio in all the experiments (we note that in the case of TA the stoichiometry is an estimate only because the structure shown in Fig. 1c is an idealized one). For selected cases, *in situ* gelation by injection was demonstrated by preparing buffer solutions of 100 mM sodium acetate/acetic acid at pHs 3.2, 4, 4.5, and 5 or 100 mM H_2CO_3/$NaHCO_3$ (pH 8.4 and 9.9). A precursor solution of 8.3 mg PEG8H-BA4 and polyphenol (0.5 mg EA or 0.7 mg EGCG) in 25 μL DMSO was injected into 10 mL of the buffers listed above and the gelation process was recorded in videos.

Hydrogel characterization

Rheological properties of hydrogels were measured with a frequency sweep test (0.6 rad s^{-1} to 60 rad s^{-1} at 25 °C) using a MCR 302 Modular Compact Rheometer (Anton Paar, Ashland, VA) with a parallel plate geometry (8 mm diameter). The crossover frequencies of storage (G') and loss (G'') moduli, as well as the G' values at 30 rad s^{-1} of each hydrogel was recorded. Qualitative stability of the gels in buffer was measured by immersing them in excess pH 7.4 PBS buffer at 37 °C. The buffer was replaced every day and the persistence of the hydrogel was confirmed visually.

AFM single molecule force spectroscopy

Glass coverslips (VWR) were cleaned in Piranha solution (H_2SO_4/H_2O_2 70 : 30 v/v, caution: care must be taken when using Piranha solution) at room temperature for 1 hour and then rinsed extensively with Milli-Q water followed by rinsing with ethanol and dried under a stream of nitrogen gas. AFM cantilevers were also cleaned using a similar method.[46] Polyphenols were dissolved and mixed with a solution of PEG-BA in buffer (pH 8.4 or 9.9); several drops (50–100 μL) of the mixture were pipetted onto glass coverslips and allowed to adsorb at room temperature for 30 minutes. The coverslips were then rinsed with buffered water and used immediately in SMFS experiments. Measurements were carried out using a JPK ForceRobot 300 (JPK Instruments AG, Germany) with a tip velocity of 2000 nm s^{-1} over a z-piezo distance of 400 nm. Cantilevers (MLCT from Bruker Nano Inc.) of typical spring constant of 30–60 pN nm^{-1} were used for all experiments and calibrated using the equipartition theorem.[47,48] The force-extension traces were recorded and analyzed using data processing software from JPK.

Drug release measurement

50 mg of PEG and 3 mg of EA were dissolved in 150 μL of DMSO and 50 μL of this solution was then injected into 40 mL of pH 7.4 PBS buffer to form a hydrogel. At each time point the container was centrifuged at 4000 rpm for 5 minutes and the supernatant was removed, saved for analysis, and replaced with an equal volume of the fresh PBS buffer. This procedure was carried out after the first hour and on a daily basis afterwards. The amount of EA released was measured by High Performance Liquid Chromatography (HPLC) using an Agilent Technologies 1260 Infinity instrument. The standard curve of EA was measured in solutions of known EA concentrations in 10% DMSO, 90% acetonitrile (Fig. S11†).

In vitro cytotoxicity

Human oral cancer cell line CAL-27 was used to test the *in vitro* anticancer properties of PEG8H-BA4-EA hydrogel. The measured LC50 value of EA for CAL-27 cells was 2.89 ± 0.3 μg mL^{-1} (Fig. S12†). CAL-27 cells were seeded onto 6-well plates and cultured in DMEM buffer with 10% fetal bovine serum (FBS) to reach a concentration of 10^5 cells per ml. Then the cell culture media was replaced with 3 ml 5% FBS DMEM solution and a transwell was added on top of each well. Each of the following formulations was analyzed by the transwell experiment: 50 μL DMSO solution of 17 mg PEG8H-BA4 and 1 mg EA; 50 μL DMSO solution of 1 mg EA; 50 μL DMSO solution of 17 mg PEG8H-BA4 and 50 μL DMSO. An untreated control group was also performed by placing an empty transwell in the well. The cells were incubated in 5% CO_2 at 37 °C incubator for two days before they were stained with ReadyProbes® cell viability image kit blue/green (Molecular Probes) for 15 minutes. After the staining, the cells were imaged using life technologies EVOS FL fluorescence microscope at DAPI (blue, live cells) and GFP (green, dead cells) channels (Fig. S13†). The survival rate of the cells was calculated based on image analysis using ImageJ.

Results and discussion

Boronic acid polymer design

The equilibrium between boronic acid and diol is highly influenced by the pH.[36–39,49] Formation of boronate ester bonds is dependent on the pK_as of both boronic acid and diol molecules and is usually facilitated at higher pH values, often above pH 8. Through the use of chemically modified boronic acids,[39,41,43–45] it is possible to shift the pK_a to lower values and therefore drive complex formation and hydrogel stability at neutral or even slightly acidic pH. Here we exploited this strategy with branched PEGs modified with boronic acids of variable pK_a values (Fig. 1), combining these with naturally derived polyphenols to form hydrogels.

Hydrogel formation

A structural requirement guiding the selection of cross-linkers used in this study was that they should contain at least two sites for boronate ester formation, *i.e.* a combination of aromatic *ortho*-dihydroxyl groups and alkyl *cis*-diol (Fig. 1c and S14, Table S1†). Only compounds that meet this criterion would be expected to form networks by cross-linking polymers *via* boronate ester complex formation. Studies of PEG-BAs and polyphenols utilized visual inspection to quickly screen for compositions that formed gels at pH 7.4. We initially surveyed six PEG-BAs consisting of both four-arm (PEG4P) and eight-arm (PEG8T and PEG8H) polymers terminated with the four phenyl boronic acids (BA1–BA4) as shown in Fig. 1. These polymers were mixed with over 20 polyphenols, saccharides, antibiotics and dyes (Table S1 and Fig. S14†) and examined for evidence of gel formation. Visual surveys of these combinations revealed EGCG, EA, TA, RT, RA and CA as gel-forming linkers under these conditions. Other compounds listed in Table S1† did not show evidence of gel formation and were not investigated further.

Hydrogel characterization

The influence of polymer architecture and boronic acid pK_a was revealed in rheology experiments using EGCG as a model cross-linker in pH 7.4 buffer (Table 1, Fig. 2 and S15†). Typically, a low crossover frequency along with high plateau G' values are indicators of a stiffer hydrogel. The rheology results reveal the dynamics of boronate ester complexes and expected trends in hydrogel stability when the pK_a value of boronic acid is changed. For example, in the case of the 4-arm PEG system, boronic acid BA1 (pK_a 9.0) had a significantly higher crossover frequency when compared to BA2 (pK_a 7.6) and BA3 (pK_a 7.2).

Additionally, the effect of polymer architecture is apparent from the low crossover frequency and high plateau storage modulus of 8-arm PEG polymers compared to 4-arm PEGs with equivalent boronic acid composition, likely due to higher crosslinking density. The influence of hexaglycerol (H) *versus* tripentaerythritol (T) core in 8-arm PEG-BAs was more subtle, as PEG8H-BA4-EGCG and PEG8T-BA4-EGCG hydrogels both had similar rheological behavior.

Most importantly, PEG8H-BA4 resulted in the lowest crossover frequencies and highest plateau G' value among all of the hydrogels tested. Therefore, we selected PEG8H-BA4 for further characterization. Using PEG8H-BA4 as a polymer platform, we then conducted a more in-depth study of polyphenol cross-linkers by comparing the rheological properties and physiologic stability of hydrogels made from PEG8H-BA4 with EGCG, EA, TA, RT, RA, NDGA and CA (Table 2 and Fig. S16†). Hydrogels formed with EGCG, TA, or EA were stable for more than two months in excess pH 7.4 PBS buffer, while gels formed with other linkers were completely dissolved over the course of several days. In the case of EA, attempts to make hydrogels by mixing solutions of PEG8H-BA4 and EA in the PBS buffer were confounded by the poor solubility of EA at pH 7.4,[50] forming precipitates of EA. We therefore employed DMSO as a solvent for EA; gels formed by injecting a DMSO solution of EA into a PBS solution of PEG8H-BA4 at pH 7.4 maintained their integrity in physiological condition for several months.

Table 1 Rheological properties of hydrogels formed from EGCG and boronic acid functionalized PEGs

Hydrogel composition	Crossover frequency (rad s^{-1})	G' at 30 rad s^{-1} (Pa)
PEG4P-BA1-EGCG	19.67	2.3×10^4
PEG4P-BA2-EGCG	2.72	1.1×10^4
PEG4P-BA3-EGCG	7.70	1.4×10^4
PEG8T-BA3-EGCG	3.52	4.8×10^4
PEG8T-BA4-EGCG	0.90	2.6×10^4
PEG8H-BA4-EGCG	0.86	5.2×10^4

Single molecule force spectroscopy

The SMFS technique has been recognized as a unique tool that enables researchers to study molecular features of noncovalent and dynamic covalent bond interactions in macromolecules.[51–53] Previous SMFS reports have shown the power of this method to study mechanical properties of proteins such as unfolding events of globular modules at the molecular level.[54–57] SMFS was performed here in order to provide more insight into molecular phenomena underlying the observed macroscopic behavior. To the best of our knowledge no molecular scale SMFS studies on the strength, reversibility, and pH dependence of these interactions have been

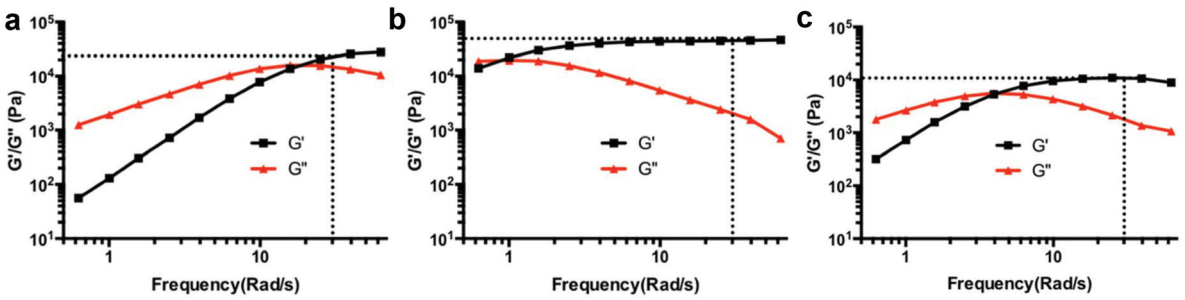

Fig. 2 Results of rheology frequency sweep test for hydrogels cross-linked with EGCG and EA at pH 7.4. (a) PEG4P-BA1-EGCG; (b) PEG8H-BA4-EGCG; (c) PEG8H-BA4-EA. G' and G'' represent storage and loss moduli, respectively. The storage moduli at 30 rad s^{-1} are marked.

Table 2 Rheological properties and stabilities of hydrogels formed from PEG8H-BA4 and selected polyphenol cross-linkers in PBS buffer at pH 7.4

Crosslinker	Solvent[a]	Stability	ω^b (rad s^{-1})	G' at[c] (Pa)
Epigallocatechin gallate (EGCG)	H_2O	>60 days	0.86	5.2×10^4
Ellagic acid (EA)	DMSO[d]	>60 days	4.07	1.3×10^4
Tannic acid (TA)	H_2O	>60 days	0.70	5.5×10^4
Nordihydroguaiaretic acid (NDGA)	H_2O/DMSO	24 hours	5.49	2.2×10^4
Rutin trihydrate (RT)	H_2O/DMSO	24 hours	22.5	1.6×10^4
Rosmarinic acid (RA)	H_2O/DMSO	24 hours	4.44	2.5×10^4
Carminic acid (CA)	H_2O/DMSO	24 hours	3.51	5.1×10^4

[a] Limited solubility of some linkers required the use of DMSO or a H_2O/DMSO cosolvent. [b] Crossover frequency. [c] G' at 30 rad s^{-1}. [d] PEG8H-BA4-EA formed through *in situ* gelation.

reported. We applied the recently developed "multiple-fish-hook" approach,[58,59] which is based on establishing strong interactions between the polymer backbone and the substrate through physisorption and randomly picking up molecules by an unmodified cantilever, as shown schematically in Fig. 3. Using this method, we were able to probe the molecular mechanics of the boronate ester complexes formed between PEG8H-BA4 and polyphenol linker molecules at neutral and alkaline pH as indicated by a "sawtooth" pattern, reminiscent of what is observed upon unfolding of a globular protein under stretch,[54–57] in the *F–D* curves (Fig. 3 and S17†). Nonspecific adsorption of polymer to the cantilever followed by retraction revealed multiple sequential dissociation events due to the multivalent nature of the polymers.

Each individual dissociation event is preceded by force-induced polymer chain extension, culminating in boronate ester bond rupture, which in turn reveals previously unloaded polymer chain segments (the so-called "hidden length"), followed by further chain extension and subsequent rupturing of additional boronate ester linkages. A worm-like chain model was used to fit the unbinding events (Fig. 3b and S17†), yielding a persistence length of ~0.4 nm, consistent with the value for a single PEG chain reported in literature.[60] This suggests that the rupture forces measured for those peaks corresponded

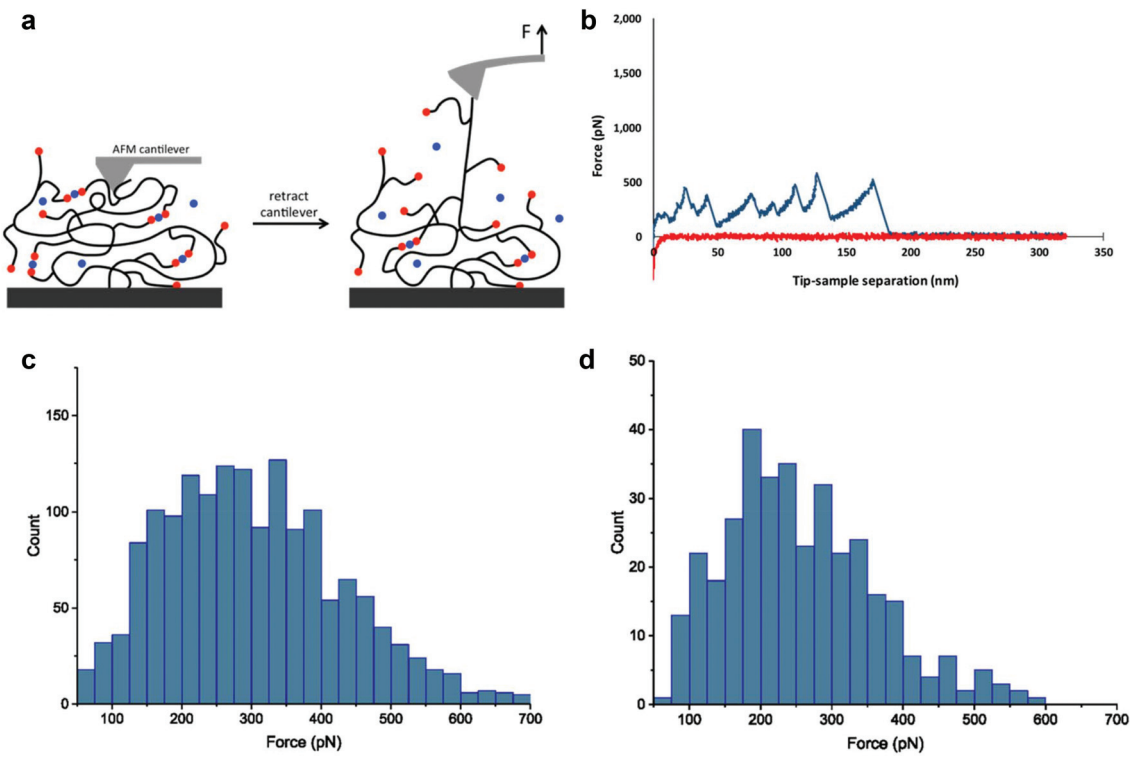

Fig. 3 Single molecule force spectroscopy experiments. Schematic of the experiments is shown in (a) with boronic acids in red and polyphenols in blue. Polymer chains are picked up through physical adsorption to the cantilever tip. Retraction of the cantilever from the surface results in sequential rupture of boronate ester cross-links which gives rise to a sawtooth-like pattern in the force–distance curve. A representative force-separation curve of PEG8H-BA4-EGCG is shown in (b), with approach curve shown in red and retraction curve in blue. The force histograms of PEG8H-BA4-EGCG and PEG8H-BA4-EA interactions are shown in (c) and (d), respectively.

to single molecule interactions; the histograms of these values have been plotted in Fig. 3c and d. Clearly, the mechanical stability of the dynamic covalent boronate ester bonds is higher than most noncovalent interactions, such as streptavidin–biotin[61] and antibody–antigen interactions,[62] similar to many metal chelation bonds,[59,63,64] but weaker than typical covalent bonds.[65] Therefore, boronate ester bonds are expected to provide strong intermolecular cross-linking of branched polymers to form mechanically stable hydrogels.

In scatter plots of distance to rupture *versus* rupture force (Fig. S18†) representing the accumulation of many experiments, we observed an interesting feature that has not been previously reported in the literature for SMFS of branched polymer systems. Inspection of the data clearly shows evidence of clustering of rupture events at separation distances of 42, 84, and 136 nm (calculated values corresponding to Fig. S18a†). Interestingly, the approximately 42 nm separation is essentially the same as the calculated average contour length of the PEG8H-BA4 polymer used in the SMFS experiments (details in ESI†). Within each cluster there can be seen a distribution of pull-off distances reflecting the statistical nature of the polymer. We therefore interpret the clustering of SMFS data as consistent with the molecular weight and architecture of the polymer chain that is being pulled by the cantilever, where increments of one or more PEG8H-BA4 molecules cross-linked by polyphenol bridge the cantilever and the flat surface. These data further confirm the single molecule nature of the measurements of polymer-polyphenol dissociation.

Among all the linker molecules used in the SMFS experiments, EGCG resulted in the highest mean dissociation force in the histogram of force distribution, followed by NDGA and EA (Table S3†). In addition, the probability of observing multiple rupture events was higher for EGCG compared to NDGA and EA. As discussed above and shown in Fig. S16,† hydrogels formed with EGCG have the lowest crossover frequency whereas larger values are associated with hydrogels formed with NDGA and EA. When considering the force values obtained in SMFS and taking into account the probability of observing rupture of interactions, which in fact correlates to extent of formation of such interactions, results obtained in the single molecule force measurements were in agreement with the data collected in rheology tests performed on the hydrogels formed with these linkers.

Consistent with the equilibrium described above and our general observations that aqueous mixtures of PEG-BAs and polyphenols are liquids at low pH due to a shift in the equilibrium to the dissociated state, we expected a low observation rate of boronate ester in SMFS experiments conducted at low pH values. Indeed, the pH-dependence of these interactions was confirmed in SMFS experiments, where at low pH no sawtooth pattern was observed for either EA or EGCG in thousands of force–distance curves analyzed, indicating that the complexes were not formed (data not shown). This pH dependent behavior was exploited for *in situ* gelation by injecting a slightly acidic PEG8H-BA4 and polyphenol solution into pH 7.4 PBS buffer (Fig. 4, gelation video in ESI†). We found both

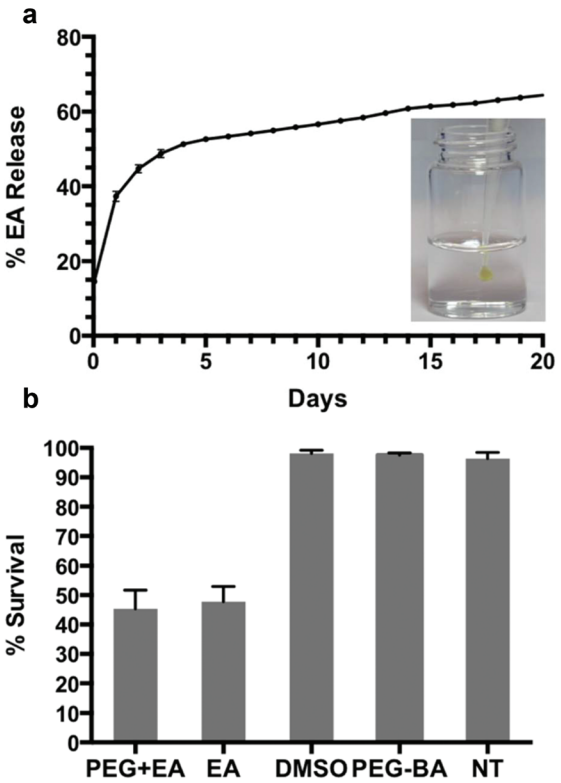

Fig. 4 The release of EA from PEG8H-BA4-EA hydrogel (a); a steady state release of 0.8% per day was observed after day 6. Inset shows a photograph of *in situ* gel formation upon injection of an acidic precursor solution of PEG8H-BA4 and EA into excess buffer at pH 7.4. CAL-27 cell survival rate upon exposure to PEG8H-BA4-EA gel (b). Similar survival rates were observed for both PEG8H-BA4-EA and EA groups, whereas nearly 100% survival was found for the DMSO, PEG8H-BA4, and untreated (NT) groups.

EA and EGCG mixed with PEG8H-BA4 can gelate upon injection into the same PBS buffer (Table S2†), which offers the opportunity to use an injectable hydrogel for localized delivery of bioactive polyphenols.

Drug release and *in vitro* cytotoxicity

Aside from playing a crucial role in pH dependent *in situ* gelation, the dynamics of boronate ester covalent bonds allow for self-healing of the hydrogel matrix,[36,66] and the opportunity for gradual release of bioactive linker and dissolution of the hydrogel. To further explore the possibility of using PEG8H-BA4 based hydrogel for drug delivery, drug release and *in vitro* cytotoxicity experiments were performed on PEG8H-BA4-EA hydrogel. One advantage of EA as a hydrogel cross-linker is its high stability toward oxidation, as EGCG and TA are more susceptible to oxidation resulting in difficulties in maintaining structural integrity and bioactivity of the hydrogel.[67–69] Additionally, the antiproliferative properties of EA have led to *in vitro* and *in vivo* investigations for cancer treatment,[12–16,70] however its poor solubility in aqueous solution limits its bioavailiability and makes delivery challenging.[50] In our system, the poor solubility of EA was overcome

by complexation with boronic acid functionalized polymer, thus providing a means for rapid formation of a polymer hydrogel that acts as a depot for gradual delivery of EA.

The release of EA from the hydrogel made by *in situ* gelation of PEG8H-BA4 and EA was measured over a 20-day period (Fig. 4). After 20 days of release, 65% of initial EA was released into the environment, 24% was found to remain in the hydrogel matrix, and the remaining 11% EA was unrecovered, possibly due to small fragments of hydrogel being washed away when the buffer solution was exchanged every day. Following an initial period of burst release, steady state release of approximately 0.8% every day was observed after day 6. We suspect that two general mechanisms play roles in the kinetic release of EA from the hydrogel matrix: the burst release of unbound EA molecules that are physically trapped in the hydrogel matrix, and the dissociation of dynamic covalent boronate ester bonds.[37,38] During the fast *in situ* gelation, the viscosity of the solution increases rapidly, causing some free EA molecules to become physically trapped in the gel matrix without reacting with BA. We suspect that these unbound molecules are responsible for the initial rapid discharge of EA. After several days of immersion in pH 7.4 PBS buffer, most of the free EA molecules are cleared and the mode governing discharge of EA switches to steadfast dynamic boronate ester bond dissociation (Fig. 4). Since our experiments were conducted under sink conditions, the low concentration of EA in the surrounding environment drives a continuous release of the EA molecules from the matrix through slow boronate ester bond dissociation.

Finally, the anticancer bioactivity of EA released from *in situ* formed gels was assayed by exposing CAL-27 cells to PEG8H-BA4-EA gel in a transwell format. Fluorescence microscopy images of stained cells under different treatment conditions are shown in Fig. S13.† Five experimental groups were established to examine the cytotoxicity of the hydrogels developed. For each group, images were taken at different spots in the sample and cell survival was calculated by image analysis (Fig. 4 and S13†). Based on the results, hydrogel-bound and free EA molecules behave quite similarly in terms of cytotoxicity, resulting in CAL-27 oral cancer cell survival rate of approximately 45% after exposure to either free EA or PEG8H-BA4-EA hydrogel. Conversely, in other experiments using only DMSO or PEG8H-BA4, no apparent cell death was observed. Due to the promising injectable physical characteristics and the biological response of cancer cells to EA released from the hydrogels, we believe that injectable boronate polymer-EA hydrogels are candidates for further study in the context of cancer therapy.

Conclusions

The PEG-BA polymers synthesized here can be utilized in combination with several natural polyphenols as *in situ* forming injectable hydrogels. The polymer gel is held together by dynamic boronate ester bonds formed spontaneously at physiologic pH. Among the polyphenol linkers investigated in this study, ellagic acid (EA), epigallocatechin gallate (EGCG) and tannic acid (TA) were capable of forming stable hydrogels in physiological condition, and PEG8H-BA4-EA hydrogel in particular displayed potential for *in situ* gelation for oral cancer treatment. In addition to reports on bioactivity of EA, there have been many studies on the possible therapeutic effects of TA and EGCG. Thus, the concept of hydrogel networks exploiting these molecules as dual cross-linker and therapeutic may lead to additional possibilities.

Conflicts of interest

There are no conflicts to declare.

Acknowledgements

The authors acknowledge support from NIH grant R37 DE014193 and NSFC grant 21522402. P. B. acknowledges postdoctoral fellowship support from the Swiss National Science Foundation (Project 151860). We also thank Dr Xi Xie of Hainan University for her help with *in vitro* cell studies.

References

1 E. Haslam, *Practical polyphenolics : from structure to molecular recognition and physiological action*, Cambridge University Press, Cambridge, UK, New York, NY, USA, 1998.
2 S. Quideau, D. Deffieux, C. Douat-Casassus and L. Pouysegu, *Angew. Chem., Int. Ed.*, 2011, **50**, 586–621.
3 T. S. Sileika, D. G. Barrett, R. Zhang, K. H. A. Lau and P. B. Messersmith, *Angew. Chem., Int. Ed.*, 2013, **52**, 10766–10770.
4 H. Ejima, J. J. Richardson, K. Liang, J. P. Best, M. P. van Koeverden, G. K. Such, J. Cui and F. Caruso, *Science*, 2013, **341**, 154–157.
5 H. Ejima, J. J. Richardson and F. Caruso, *Nano Today*, 2017, **12**, 136–148.
6 D. G. Barrett, T. S. Sileika and P. B. Messersmith, *Chem. Commun.*, 2014, **50**, 7265–7268.
7 M. Kampa, A. P. Nifli, G. Notas and E. Castanas, in *Reviews of Physiology, Biochemistry and Pharmacology*, ed. S. G. Amara, E. Bamberg, B. Fleischmann, T. Gudermann, S. C. Hebert, R. Jahn, W. J. Lederer, R. Lill, A. Miyajima, S. Offermanns and R. Zechner, Springer, Berlin Heidelberg, 2007, pp. 79–113.
8 F. D. Domenico, C. Foppoli, R. Coccia and M. Perluigi, *Biochim. Biophys. Acta, Mol. Basis Dis.*, 2012, **1822**, 737–747.
9 D. G. Nagle, D. Ferreira and Y.-D. Zhou, *Phytochemistry*, 2006, **67**, 1849–1855.
10 B. N. Singh, S. Shankar and R. K. Srivastava, *Biochem. Pharmacol.*, 2011, **82**, 1807–1821.
11 D. A. Vattem and K. Shetty, *J. Food Biochem.*, 2005, **29**, 234–266.

12 V. Arulmozhi, K. Pandian and S. Mirunalini, *Colloids Surf., B*, 2013, **110**, 313–320.
13 C. Bell and S. Hawthorne, *J. Pharm. Pharmacol.*, 2008, **60**, 139–144.
14 B. A. Narayanan, O. Geoffroy, M. C. Willingham, G. G. Re and D. W. Nixon, *Cancer Lett.*, 1999, **136**, 215–221.
15 N. P. Seeram, L. S. Adams, S. M. Henning, Y. Niu, Y. Zhang, M. G. Nair and D. Heber, *J. Nutr. Biochem.*, 2005, **16**, 360–367.
16 N. Wang, Z.-Y. Wang, S.-L. Mo, T. Y. Loo, D.-M. Wang, H.-B. Luo, D.-P. Yang, Y.-L. Chen, J.-G. Shen and J.-P. Chen, *Breast Cancer Res. Treat.*, 2012, **134**, 943–955.
17 M. C. Roberts, M. C. Hanson, A. P. Massey, E. A. Karren and P. F. Kiser, *Adv. Mater.*, 2007, **19**, 2503–2507.
18 L. He, D. E. Fullenkamp, J. G. Rivera and P. B. Messersmith, *Chem. Commun.*, 2011, **47**, 7497–7499.
19 J. A. Burdick and W. L. Murphy, *Nat. Commun.*, 2012, **3**, 1269.
20 V. Yesilyurt, M. J. Webber, E. A. Appel, C. Godwin, R. Langer and D. G. Anderson, *Adv. Mater.*, 2016, **28**, 86–91.
21 Y. Dong, W. Wang, O. Veiseh, E. A. Appel, K. Xue, M. J. Webber, B. C. Tang, X.-W. Yang, G. C. Weir, R. Langer and D. G. Anderson, *Langmuir*, 2016, **32**, 8743–8747.
22 A. P. Bapat, D. Roy, J. G. Ray, D. A. Savin and B. S. Sumerlin, *J. Am. Chem. Soc.*, 2011, **133**, 19832–19838.
23 J. L. Guo, H. L. Sun, K. Alt, B. L. Tardy, J. J. Richardson, T. Suma, H. Ejima, J. W. Cui, C. E. Hagemeyer and F. Caruso, *Adv. Healthcare Mater.*, 2015, **4**, 1796–1801.
24 S. H. Hong, S. Kim, J. P. Park, M. Shin, K. Kim, J. H. Ryu and H. Lee, *Biomacromolecules*, 2018, DOI: 10.1021/acs.biomac.8b00144.
25 J. N. Cambre and B. S. Sumerlin, *Polymer*, 2011, **52**, 4631–4643.
26 R. J. Weir and R. S. Fisher, *Toxicol. Appl. Pharmacol.*, 1972, **23**, 351–354.
27 C. H. Linden, A. H. Hall, K. W. Kulig and B. H. Rumack, *J. Toxicol., Clin. Toxicol.*, 1986, **24**, 269–279.
28 D. Roy, J. N. Cambre and B. S. Sumerlin, *Chem. Commun.*, 2009, 2106–2108.
29 J. Su, F. Chen, V. L. Cryns and P. B. Messersmith, *J. Am. Chem. Soc.*, 2011, **133**, 11850–11853.
30 P. C. Trippier and C. McGuigan, *Med. Chem. Commun.*, 2010, **1**, 183–198.
31 W. L. A. Brooks and B. S. Sumerlin, *Chem. Rev.*, 2016, **116**, 1375–1397.
32 W. Yang, X. Gao and B. Wang, *Med. Res. Rev.*, 2003, **23**, 346–368.
33 O. R. Cromwell, J. Chung and Z. Guan, *J. Am. Chem. Soc.*, 2015, **137**, 6492–6495.
34 C. Kim, H. Ejima and N. Yoshie, *RSC Adv.*, 2017, **7**, 19288–19295.
35 Y. Guan and Y. Zhang, *Chem. Soc. Rev.*, 2013, **42**, 8106–8121.
36 C. C. Deng, W. L. A. Brooks, K. A. Abboud and B. S. Sumerlin, *ACS Macro Lett.*, 2015, **4**, 220–224.
37 S. Lascano, K.-D. Zhang, R. Wehlauch, K. Gademann, N. Sakai and S. Matile, *Chem. Sci.*, 2016, **7**, 4720–4724.
38 S. J. Rowan, S. J. Cantrill, G. R. L. Cousins, J. K. M. Sanders and J. F. Stoddart, *Angew. Chem., Int. Ed.*, 2002, **41**, 898–952.
39 J. Yan, G. Springsteen, S. Deeter and B. Wang, *Tetrahedron*, 2004, **60**, 11205–11209.
40 L. He, D. E. Fullenkamp, J. G. Rivera and P. B. Messersmith, *Chem. Commun.*, 2011, **47**, 7497–7499.
41 A. Adamczyk-Woźniak, K. M. Borys, I. D. Madura, A. Pawełko, E. Tomecka and K. Żukowski, *New J. Chem.*, 2013, **37**, 188–194.
42 D. G. Hall, *Structure, properties, and preparation of boronic acid derivatives. Overview of their reactions and applications*, John Wiley & Sons, Weinheim, Germany, 2006.
43 L. P. Hammett, *J. Am. Chem. Soc.*, 1937, **59**, 96–103.
44 Y. Kim, S. A. Hilderbrand, R. Weissleder and C. H. Tung, *Chem. Commun.*, 2007, 2299–2301.
45 J. W. Tomsho, A. Pal, D. G. Hall and S. J. Benkovic, *ACS Med. Chem. Lett.*, 2012, **3**, 48–52.
46 Y.-S. Lo, N. D. Huefner, W. S. Chan, P. Dryden, B. Hagenhoff and T. P. Beebe, *Langmuir*, 1999, **15**, 6522–6526.
47 J. Lübbe, M. Temmen, P. Rahe, A. Kühnle and M. Reichling, *Beilstein J. Nanotechnol.*, 2013, **4**, 227–233.
48 J. L. Hutter and J. Bechhoefer, *Rev. Sci. Instrum.*, 1993, **64**, 1868–1873.
49 G. Springsteen and B. Wang, *Tetrahedron*, 2002, **58**, 5291–5300.
50 I. Bala, V. Bhardwaj, S. Hariharan and M. R. Kumar, *J. Pharm. Biomed. Anal.*, 2006, **40**, 206–210.
51 A. Janshoff, M. Neitzert, Y. Oberdörfer and H. Fuchs, *Angew. Chem., Int. Ed.*, 2000, **39**, 3212–3237.
52 X. Zhang, C. Liu and Z. Wang, *Polymer*, 2008, **49**, 3353–3361.
53 H. Clausen-Schaumann, M. Seitz, R. Krautbauer and H. E. Gaub, *Curr. Opin. Chem. Biol.*, 2000, **4**, 524–530.
54 M. S. Z. Kellermayer, C. Bustamante and H. L. Granzier, *Biochim. Biophys. Acta, Bioenerg.*, 2003, **1604**, 105–114.
55 M. Carrion-Vazquez, A. F. Oberhauser, S. B. Fowler, P. E. Marszalek, S. E. Broedel, J. Clarke and J. M. Fernandez, *Proc. Natl. Acad. Sci. U. S. A.*, 1999, **96**, 3694–3699.
56 Y. Cao and H. Li, *Nat. Mater.*, 2007, **6**, 109–114.
57 D. Sharma, O. Perisic, Q. Peng, Y. Cao, C. Lam, H. Lu and H. Li, *Proc. Natl. Acad. Sci. U. S. A.*, 2007, **104**, 9278–9283.
58 X. Han, M. Qin, H. Pan, Y. Cao and W. Wang, *Langmuir*, 2012, **28**, 10020–10025.
59 Y. Li, M. Qin, Y. Li, Y. Cao and W. Wang, *Langmuir*, 2014, **30**, 4358–4366.
60 W. Ott, M. A. Jobst, M. S. Bauer, E. Durner, L. F. Milles, M. A. Nash and H. E. Gaub, *ACS Nano*, 2017, **11**, 6346–6354.
61 F. Rico and V. T. Moy, *J. Mol. Recognit.*, 2007, **20**, 495–501.
62 P. Hinterdorfer, W. Baumgartner, H. J. Gruber, K. Schilcher and H. Schindler, *Proc. Natl. Acad. Sci. U. S. A.*, 1996, **93**, 3477–3481.

63 K. M. Im, T. W. Kim and J. R. Jeon, *ACS Biomater. Sci. Eng.*, 2017, **3**, 628–636.
64 H. Lee, N. F. Scherer and P. B. Messersmith, *Proc. Natl. Acad. Sci. U. S. A.*, 2006, **103**, 12999–13003.
65 J. Ribas-Arino and D. Marx, *Chem. Rev.*, 2012, **112**, 5412–5487.
66 S. Kim, S. K. Nishimoto, J. D. Bumgardner, W. O. Haggard, M. W. Gaber and Y. Yang, *Biomaterials*, 2010, **31**, 4157–4166.
67 H. Barbucci, *Biological Properties and Applications*, Springer, 2009.
68 E. M. Daniel, A. S. Krupnick, Y.-H. Heur, J. A. Blinzler, R. W. Nims and G. D. Stoner, *J. Food Compos. Anal.*, 1989, **2**, 338–349.
69 N. Li, L. S. Taylor, M. G. Ferruzzi and L. J. Mauer, *Food Res. Int.*, 2013, **53**, 909–921.
70 S. Kim, S. K. Nishimoto, J. D. Bumgardner, W. O. Haggard, M. W. Gaber and Y. Yang, *Biomaterials*, 2010, **31**, 4157–4166.